

Influence of Fiber Wettability on the Interfacial Adhesion of Continuous Fiber-Reinforced PPESK Composite

Ping Chen,^{1,2} Chun Lu,¹ Qi Yu,¹ Yu Gao,² Jianfeng Li,¹ Xinglin Li³

¹School of Chemical Engineering, Dalian University of Technology, Liaoning 116012, China

²Center for Composite Materials, Shenyang Institute of Aeronautical Engineering, Liaoning 110034, China

³Changchun Institute of Applied Chemistry, Chinese Academy of Sciences, Jilin 130022, China

Received 11 December 2005; accepted 24 March 2006

DOI 10.1002/app.24681

Published online in Wiley InterScience (www.interscience.wiley.com).

ABSTRACT: Interfacial adhesion between fiber and matrix has a strong influence on composite mechanical performance: better interfacial adhesion can enhance composite transverse properties, flexural properties, and interlaminar shear strength, and so on. To exploit the reinforcement potential of the fibers in advanced composite, it is necessary to reach a deeper understanding on the relation between fiber wettability and interfacial adhesion. In our experiment, we study the influence of fiber wettability on interfacial properties of fiber/PPESK composites by choosing three kinds of fibers with different wettabilities. The relation

between fiber wettability and surface free energy was discussed, and the influence of fiber wettability on the interfacial property of fiber/PPESK composites was analyzed. Results indicate that higher surface free energy can enhance the wettability between fiber and matrix, and the humid resistance and interfacial adhesion can be improved at the same time. © 2006 Wiley Periodicals, Inc. *J Appl Polym Sci* 102: 2544–2551, 2006

Key words: wettability; fiber composites; interfacial; poly(phthal azione ether sulfone keton); contact angle; XPS

INTRODUCTION

Fiber-reinforced composite is composed of resin and reinforced fiber. Reinforced fiber determines the mechanical performance, and resin determines the heat resistant property, chemical corrosion resistant property, and process ability. Besides, composite mechanical performances are critically dependent on the interfacial adhesion between fiber and matrix: better interfacial adhesion can enhance composite humid resistant property, transverse property, flexural property, and interlaminar shear strength and so on. Fiber wettability has a strong influence on the interfacial adhesion between fiber and matrix: incomplete wetting may produce interfacial defects and reduce the IFSS by flaw-induced stress concentration. When fiber surface free energy is high, the contact angle between fiber and polymer solution is small, so fiber can be well impregnated by polymer solution, as a result, the flaw (voids forming during the process) can be reduced. On

the other hand, better wetting can enhance the IFSS by improving the work of adhesion, high surface energy indicates that fiber contains more polar groups on the surface, interfacial adhesion can be improved by the strong interaction between resin and the polar groups.^{1,2}

PPESK is a kind of novel thermoplastic (the structure is shown in Fig. 1), compared with traditional thermoplastic^{3–6} (such as: PEEK, PES, PEI), it has excellent thermal resistance property ($T_g = 287^\circ\text{C}$), besides it can be dissolved in usual solvents (such as DMAc, NMP, and chloroform), thus fibers-reinforced PPESK composite can be prepared through solution impregnation technique. In our experiment, we study the influence of fiber wettability on interfacial properties of fiber/PPESK composites by choosing three kinds of fibers with different wettabilities. Fiber surface chemical composition was indicated by X-ray photoelectron spectroscopy (XPS), surface free energies of the fibers were characterized by Wilhelmy method, and composite interfacial properties were indicated by humid resistance property, interfacial mechanism test, and rupture morphology analysis (SEM, scanning electron microscope).

Correspondence to: P. Chen (chenping_898@126.com).

Contract grant sponsor: National Defense 11th 5-year program Foundational Research Program; contract grant number: A352060215.

Contract grant sponsor: Liaoning Excellent Talents in University; contract grant number: 2005RC-14.

Contract grant sponsor: Natural Science Foundation of Liaoning Province; contract grant number: 20044002.

EXPERIMENTAL

Material

The matrix used in our experiment is poly(phthal azione ether sulfone ketone) (characteristic viscosity,

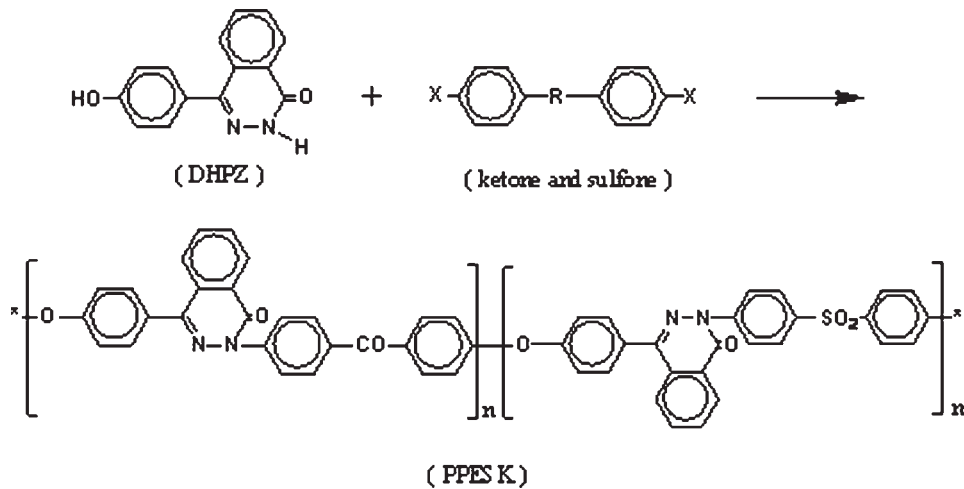


Figure 1 Structure of PPESK molecule.

$\eta = 0.35$; glass transition temperature, $T_g = 287^\circ\text{C}$).⁷⁻¹² The structure is shown in Figure 1.

From Figure 1 we can see that PPESK molecular is composed of rigid benzene and 4-(4'-hydroxyphenyl)-2,3-phthalazin-1-one (DHPZ), linked together by ether-bond and polar groups of ketonic and sulfonic. Since noncoplanar twisted aromatic structure DHPZ is introduced into the polymer backbone, the matrix is endowed with good solubility and novel thermal resistance, thus fiber-reinforced PPESK composite can be prepared through solution impregnation technique. Solvent: DMAc, solution concentration (20 wt %), high strength glass fiber (S-GF 250 dex) (dewaxing treatment); carbon fiber (Toray: T700sc); aramid fiber (Armos: F-12). The fibers used here were not treated with any methods in our laboratory except dryness. The properties of the fibers are listed in Table I.

Fiber surface element analysis

Fiber surface chemical composition was analyzed by XPS (thermo ESCALAB 250) using AlKa photo beams at normal emission angle.

Fiber wettability

Fiber wettability is the reflection of surface free energy which includes polar and dispersive component. In our experiment, surface free energy of the fibers was analyzed according to Wihelmy method, on a dynamic

contact angle analysis system (Cahn DCA-322) (as illustrated in Fig. 2):

$$F_{\text{Measured}} = F_{\text{Fiber}} - F_{\text{Buoyancy}} + F_{\text{Wetting}} \quad (1)$$

$$F_{\text{Wetting}} = \gamma_l p \cos \theta \quad (2)$$

$$\gamma_l (1 + \cos \theta) = 2 \cdot \sqrt{\gamma_s^p \gamma_l^p} + 2 \cdot \sqrt{\gamma_s^d \gamma_l^d} \quad (3)$$

$$\gamma_{\text{Total}} = \gamma_s^p + \gamma_s^d \quad (4)$$

F_{wetting} is the wetting force measured by the microbalance; p is the wetted perimeter; θ is the dynamic contact angle between fiber and liquid; γ_l is the surface tension of the testing liquid; γ_{Total} is the surface free energy of the fiber; γ_s^p is the polar component; and γ_s^d is the dispersive component.

In the experiment, a single fiber was mounted indirectly to a wire hook suspended from a microbalance and then immersed (emersed) into the test liquid by raising the elevating stage with the test liquid reservoir. The force exerted on the fiber may be expressed as the sum of the wetting, gravitational, and buoyancy force, the measured force is given as eq. (1). By moving the stage up to the fixed immersion depth at a constant speed of 1 mm/min, a typical force-high plot (y) was given schematically. The advancing and receding dynamic contact angles (θ) were calculated from eq. (2). Fiber surface energies were calculated using Owens-Wendt eqs. (3) and (4).^{1,2,13-17}

TABLE I
Property of the Fibers

Property	E (GPa)	σ_{ult} (GPa)	ϵ_{ult} (%)	ρ (g/cm ³)	Fiber diameter (μm)
Glass fiber	81.3	3.44	4.8	2.5	15
Aramid fiber (F-12)	109	4.4	3.2	1.45	15
Carbon fiber (T700sc)	230	4.9	1.5	1.8	7

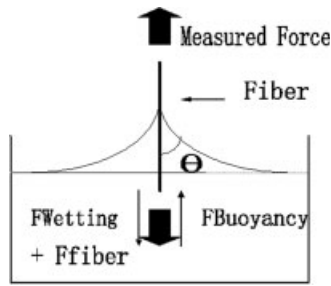


Figure 2 Schematic of dynamic contact angle measurement.

Interfacial properties and humid resistance

Preparation of fiber/PPEsk composite: PPEsk was dissolved in DMAc solvent (20 wt %) and then continuous fiber was impregnated with the low viscosity PPEsk/DMAc solution, and after removing the solvent, fiber/PPEsk composite was made by compression molding technique.^{3,18} Composite transverse property and interlaminar shear strength were carried out according to GB3354-82 and GB3357-82 on Shimadzu universal testing machine with a constant crosshead rate of 2 mm/min; at least seven specimens were tested for each of the composite studied.

Composite water absorption tests were carried as follows: composites were cut into 100 mm × 60 mm × 2 mm smaller pieces, then they were immersed into boiling water (100°C), and the increase in weight of the composites at a fixed interval time was measured. Humid resistance properties were indicated by mechanical performance that remained after the composites were immersed into boiling water (100°C) for 48 h.

Morphologies of composite interlaminar shear ruptures were characterized using a JSM-5600LV scanning electron microscope (SEM), the failure mechanisms of the composites were analyzed from the SEM pictures.

RESULTS

Surface composition

The surface chemical composition of the fibers was obtained from the fiber surface by XPS analysis (Fig. 3), and the element concentration on fiber surface were estimated from the corresponding peak areas (Table II). From Figure 3, we can see that all of the three fibers have high C (~280 eV), and O (~530 eV) content, however the O_{1s}/C_{1s} of the fibers are different, among the fibers carbon fiber has the highest O_{1s}/C_{1s} ratio (about 0.26), while aramid fiber and glass fiber are relatively lower.

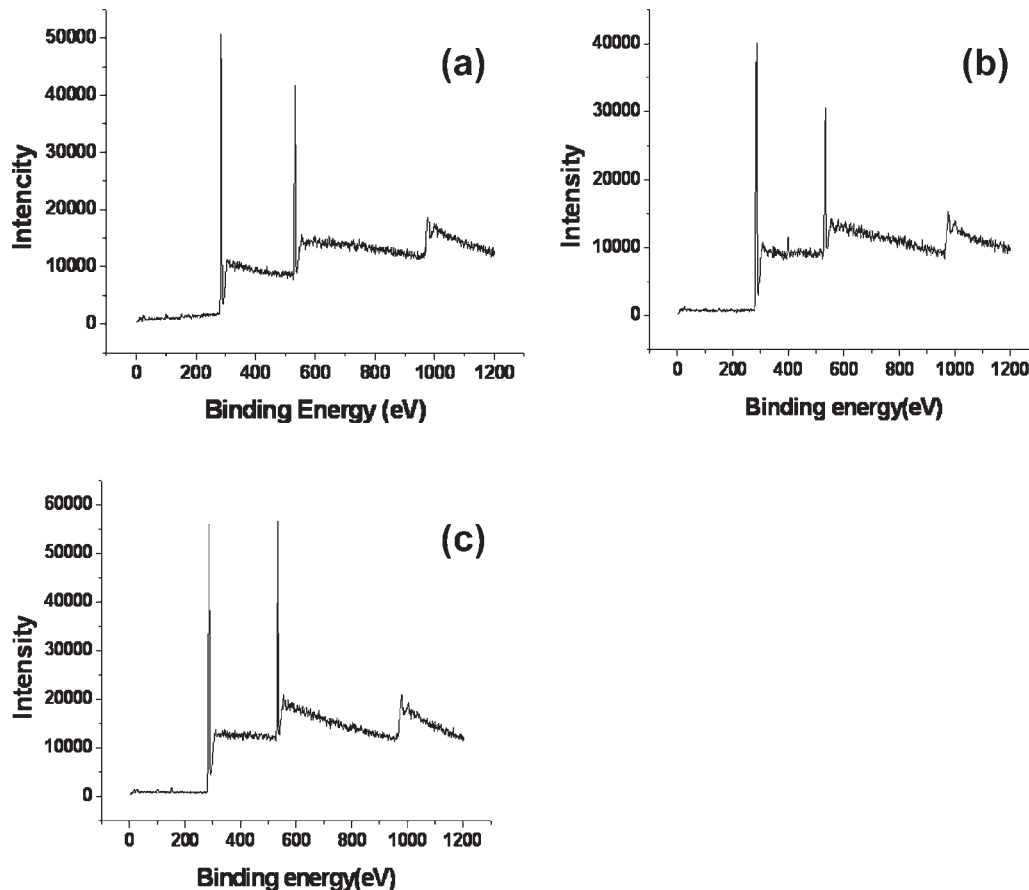


Figure 3 Surface chemical composition of the fibers (a) glass fiber; (b) aramid fiber; and (c) carbon fiber.

TABLE II
Surface Element Content of the Fibers (%)

	C	O	N	Si
Glass fiber	78.7	19.75	0	1.55
Aramid fiber	80.18	16.46	2.57	0.79
Carbon fiber	78.36	20.44	0	1.2

We take a further analysis of the functional groups ($-C-OH$ or $-C-O-R$, $C=O$, $-COOH$ or $-COOR$) on the surface of the fibers (Fig. 4), and the content of the functional groups were calculated from the peak areas (Table III). From Figure 4(a) (glass fiber), we can see that a single peak at 284 eV is due to $C-C(H)$ group (content 98.1%); small polar group can be seen on the glass fiber surface. From Figure 4(b) (aramid fiber), the peak at 283.7 eV is due to $C-C(H)$ group (58.4%), and the peak at 285.8 eV

might correspond to $-C-N-$ (39.0%); the ratio of polar/nonpolar is 0.71. From Figure 4(c) (carbon fiber), the peak at 284.5 eV is due to $C-C(H)$ group (19.4%), the peak at 286.3 might correspond to $-C-N-$ group (54.5%), and the peak at 287.5 eV is considered to be $C=O$ group of simple carbonyl compounds (26.1%), and the ratio of polar/nonpolar is 4.16. From the above analysis, we can conclude that the surface polarity of aramid fiber and carbon fiber is greater than that of glass fiber.

Surface free energy of the fiber

The contact angles were derived using a Cahn dynamic contact angles analysis system, and surface free energies were calculated using eqs. (3) and (4) and the results are listed in Table IV.

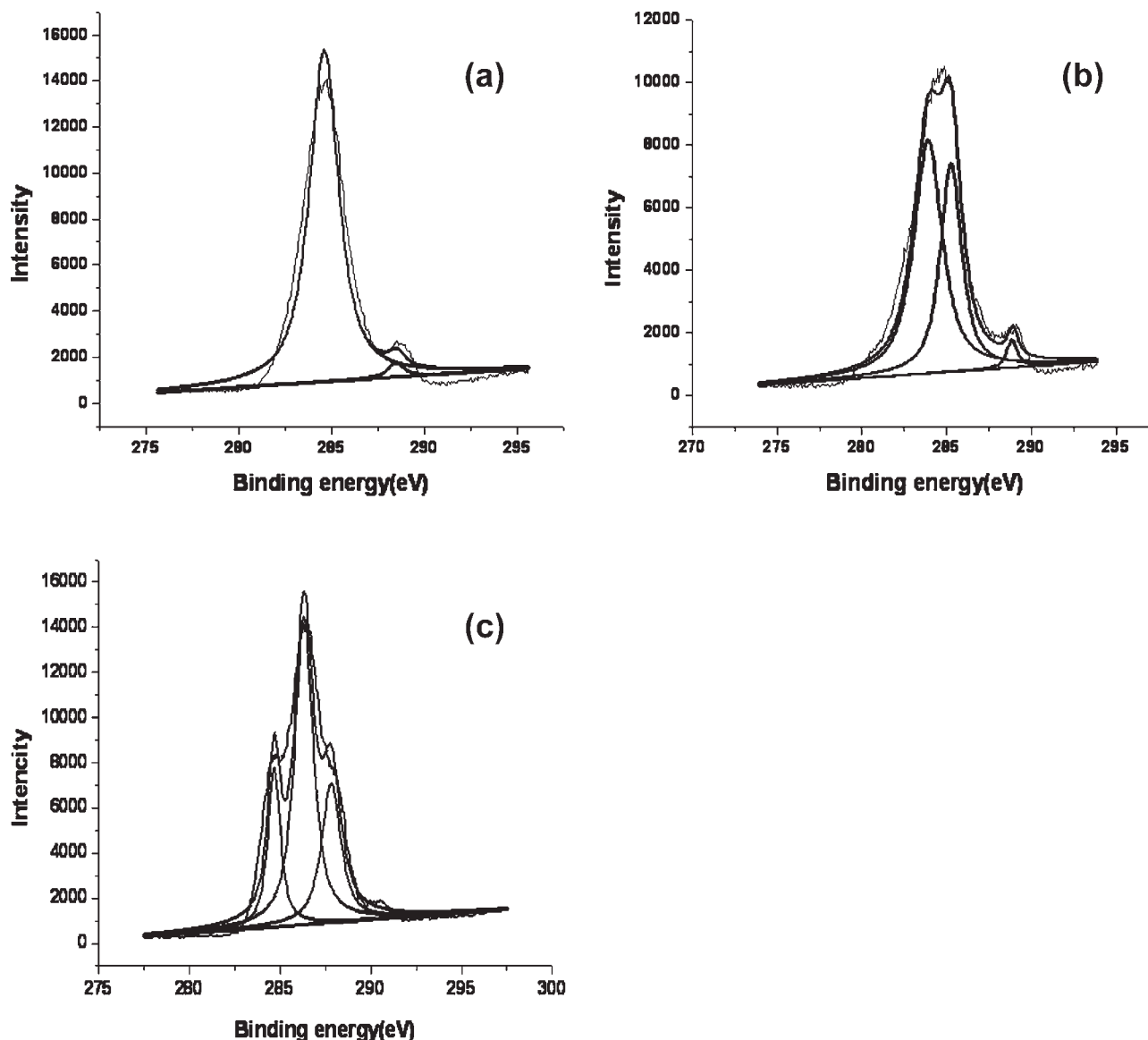
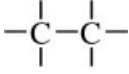
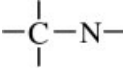
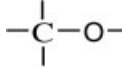
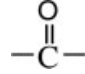
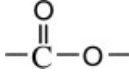


Figure 4 Surface functional groups of the fibers (a) glass fiber; (b) aramid fiber; and (c) carbon fiber.

TABLE III
Functional Groups on Fiber Surface

Fibers	Functional group (%)				
	 284 (eV)	 285.8 (eV)	 286 (eV)	 287 (eV)	 289 (eV)
Glass fiber	98.1%	0	0	0	1.9%
Aramid fiber	58.4%	39.0%	0	0	2.6%
Carbon fiber	19.4%	0	54.5%	26.1%	0

The polarity of the fiber can also be indicated by the surface free energy, which is equal to the figures of the work required to form a new unit surface when separating two phases that remain in equilibrium in a reversible isothermal process. From Table IV, we can see that the surface free energy of aramid fiber and carbon fiber are 34.6 and 38.9 mN/m, while glass fiber is only 24.2 mN/m, as can be seen the surface polarity of aramid fiber and carbon fiber is higher than that of glass fiber, the result agrees with the XPS analysis. The difference of the surface free energies is due to the different surface treatment of fibers. During fiber preparation, sizing is often used to protect fibers. Generally, glass fiber is treated with paraffin emulsion, carbon fiber is treated with diluted epoxy resin solution, and aramid fiber is mainly treated with aliphatic ester, unsaturated ester, aromatic ester, aliphatic ester salt, and amine.^{13,19,20} Though glass fiber used in our experiment has been dewaxed, substantial amount of nonpolar group can be seen from XPS analysis, so the surface free energy is low. Carbon fiber and aramid fiber have been sized, there are many polar groups on fiber surface, so the surface free energy is relatively higher.

DISCUSSION

Fiber wettability

When a drop of liquid comes into contact with an ideally smooth solid surface, a three-phase equilibrium among the solid, liquid, and vapor can be observed. The equilibrium is described by Young's equation:

$$\gamma_l \cos \theta = \gamma_s - \gamma_{sl} \quad (5)$$

Where θ is the contact angle; γ_l is the experimentally determined surface tension of the liquid; γ_s is the surface free energy of the solid, and γ_{sl} is the solid-liquid interfacial energy. Surface free energy can be divided into two parts: polar part and dispersive part.

$$\gamma = \gamma^p + \gamma^d \quad (6)$$

Polar part result from the molecule interaction due to Keesom Polar contribution (hydrogen bonding and dipole-dipole interaction etc.) and dispersive part is due to the London dispersion forces.

Solid-liquid interaction can be expressed by Owen-Wendt equation which includes polar and dispersive interactions:

$$\gamma_{sl} = \gamma_s + \gamma_l - 2(\gamma_s^p \gamma_l^p)^{1/2} - 2(\gamma_s^d \gamma_l^d)^{1/2} \quad (7)$$

The thermodynamic work of adhesion between fiber and solution (W_a) is also a measure of the interaction between two phases. It is given by the work required to separate reversibly the interface between two phases from their equilibrium to infinity. The energy balance is given by Dupre's equation:

$$W_a = \gamma_s + \gamma_l - \gamma_{sl} \quad (8)$$

By substitution of γ_{sl} in Dupre's eq. (8) by eq. (7), the work of adhesion with its polar and dispersive components becomes^{13,21}:

$$W_a = 2 \left[(\gamma_s^d \gamma_l^d)^{1/2} + (\gamma_s^p \gamma_l^p)^{1/2} \right] \quad (9)$$

From eq. (9) we can see that the thermodynamic work of adhesion (W_a) is determined by the surface

TABLE IV
The Dynamic Contact Angle and Surface Free Energy of the Fibers

Sample	Contact angle with water	Contact angle with <i>n</i> -octane	γ^p (mN/m)	γ^d (mN/m)	γ_{total} (mN/m)
Distilled water	–	–	51.0	21.8	72.8
<i>n</i> -octane	–	–	0	21.8	21.8
Glass fiber	81.2	80.0	16.7	7.5	24.2
Aramid fiber	68.2	52.8	20.6	14.0	34.6
Carbon fiber	62.7	72.8	29.8	9.1	38.9

free energy (γ) of the fibers, when surface free energy is higher the work of adhesion is bigger, as a result fibers can be well impregnated by solution. From fiber surface chemical composition and surface free energy analysis, we can see that the surface polar group of carbon fiber and aramid fiber is higher than that of glass fiber, besides the surface free energy of aramid fiber and carbon fiber is 34.6 and 38.9 mN/m, while glass fiber is only 24.2 mN/m, so the wettabilities of aramid fiber and carbon fiber are better than that of glass fiber.

Composite humid resistance property

High surface free energy can enhance fiber impregnation, as a result fiber will be adhered to resin tightly with little flaw in the interface, so composite humid resistance property can be improved. In fiber/composites, moisture absorption depends on the properties of matrix' fibers' and interfacial adhesion. In fiber/PPESK composite, both of the fibers and resin have lower water absorption, moisture permeates into composite through the interface rather than through the resin matrix or fiber. So moisture absorption can reflect the interfacial flaw of the composites indirectly.²²⁻²⁶ The moisture absorptions of three composites are indicated in Figure 5.

From Figure 5, we can see that the moisture absorption velocity of glass fiber composite is the fastest, whereas carbon fiber and aramid fiber composites are relatively slower. At the end of the experiment, glass fiber composite absorbs more water (about 1.63 wt %) than aramid fiber and carbon fiber composites (1.18 and 0.93 wt %). The fastest moisture absorption velocity of glass fiber composite indicates that moisture can permeate through the interface easily, which means that the interfacial adhesion of glass fiber and matrix is poor; while the moisture absorption velocity of carbon fiber and aramid fiber is relatively lower, which means both of the two composites have a good interfacial adhesion, and they can resist moisture permeation effectively.

When water permeates into the interface, interfacial adhesion will be destroyed or even debonded, so the

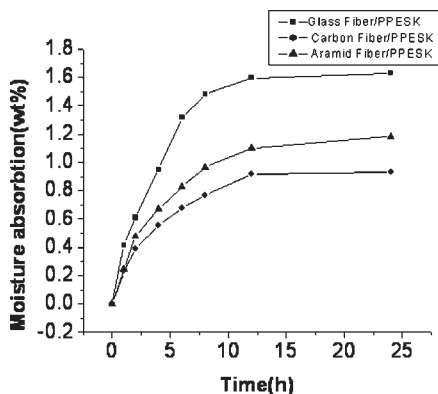


Figure 5 Moisture absorption of the composites.

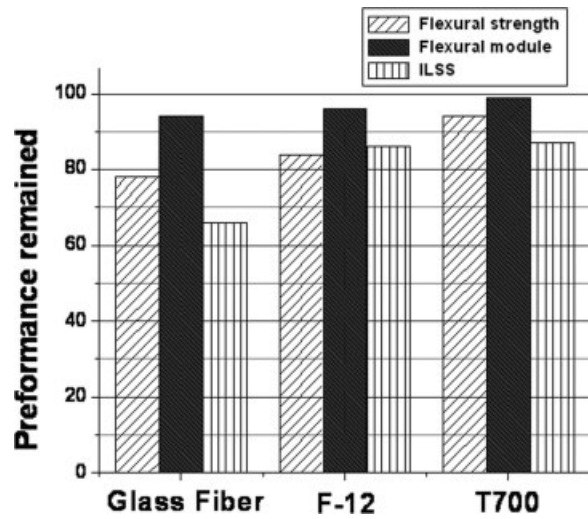


Figure 6 Humid resistant property of the composites.

mechanical performance of the composites will decrease (Fig. 6).

Figure 6 shows the mechanical performance after the composites were immersed into boiling water (100°C) for 48 h. From Figure 6, we can see that the loss of their mechanical performance is little, composites exhibit excellent humid resistant properties. However, ILSS is sensitive to humid influence, after exposing to humid condition, ILSS of aramid fiber and carbon fiber composites drops to 16 and 13%, respectively, glass fiber composite drops to 36%. The flexural strength of carbon fiber and aramid fiber composites remain 94 and 83%, and glass fiber is merely 78%. Based on the relation between interfacial adhesion and humid resistance properties, it can be concluded that the carbon and aramid fiber composites have better interfacial adhesion than glass fiber composites.

Interfacial properties of fiber/PPESK composites

When composite suffers form load, the stress distribution on the fiber and matrix satisfies the Kelly-Tyson theory.^{27,28} Based on the theory, if a constant load loads on a nonfailing fiber fragment (with a diameter D and length L), the interfacial shear stress along the fiber is given by eq. (10):

$$\tau = \frac{D\sigma}{2L} \tag{10}$$

When interfacial adhesion is strong, destruction of the composite will take place in matrix near the interface, with resin adhesive on fiber surface. While interfacial adhesion is weak, fibers will be peeled off from matrix, the fiber is clean, with little resin adhesive on the surface. The morphology of composite interlaminar shear ruptures is indicated in Figure 7.

From the photographs (Fig. 7), we can see that ruptures of different composites are obviously different.

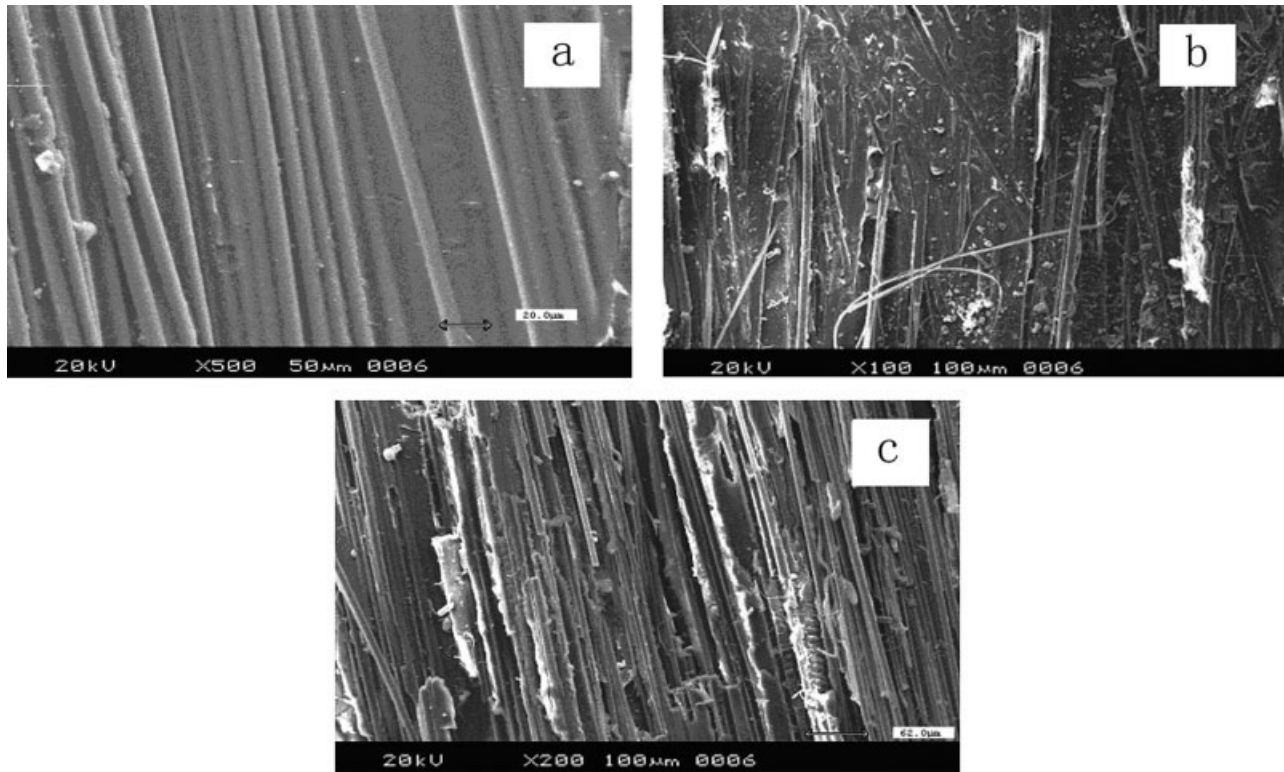


Figure 7 Morphology of interlaminar shear ruptures for (a) glass fiber; (b) aramid fiber; and (c) carbon fiber.

From the photograph of glass fiber composite [Fig. 7(a)], fibers are loosely held by matrix and the clean fiber surface indicates weak fiber/matrix interfacial adhesion, the destruction takes place on the interface between fiber and matrix. Conversely, aramid fiber and carbon fiber ruptures show [Figs. 7(b) and 7(c)] considerable matrix deformation together with fibers that are tightly held by the matrix. The primary failure mode in aramid fiber and carbon fiber composites is matrix failure. So, the interfacial adhesion of aramid fiber and carbon fiber composites are better than that of glass fiber composite.

The ILSS and transverse properties are shown in Figure 8. From the figure, we can see that the ILSS aramid fiber and carbon composites are 61.8 and 60.8 MPa, while glass fiber is only 45.0 MPa, besides, the transverse properties of aramid fiber and carbon fiber composite are relatively higher than that of glass fiber composite; aramid fiber and carbon fiber composites have better interfacial adhesion than glass fiber composite, the result agrees with our analysis above.

CONCLUSIONS

Fiber wettability has a strong influence on composite mechanical performances; surface free energies of carbon fiber and aramid fiber are higher than that of glass fiber; higher surface free energy can enhance the wettability between fiber and matrix and reduce interfacial

flaws, and the humid resistance and interfacial adhesion performance can be improved at the same time. SEM of the ruptures indicate that the primary failure mechanism of carbon fiber and aramid fiber composite is matrix failure, and glass fiber composite is interfacial failure, aramid fiber and carbon fiber composite have better interfacial adhesion than glass fiber composite. So the improvement of fiber wettability is a convenient way of improving the mechanical performance of fiber/thermoplastic composite.

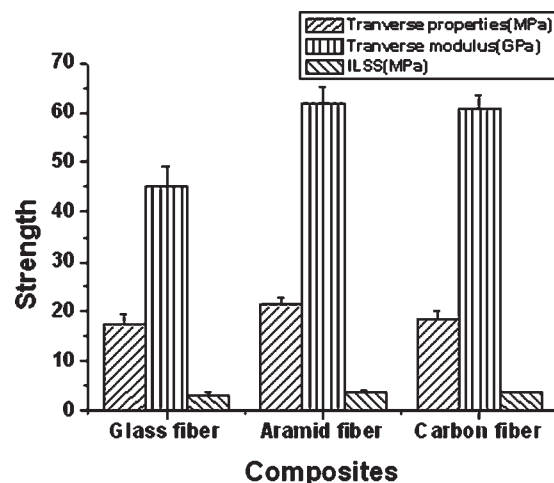


Figure 8 Transverse properties and ILSS of three different composites.

The author would like to acknowledge the valuable help given by the organizations. And acknowledgment also goes to my dear teachers Rongwen LV.

References

1. Park, J.-M.; Kim, D.-S.; Kong, J.-W. *J Colloid Interface Sci* 2002, 249, 62.
2. Luner, P. E.; Oh, E. *Colloids Surf A* 2001, 181, 31.
3. Hou, M.; Ye, L.; Mai, Y.-W. *Plast Rubber Compos Process Appl* 1995, 23, 279.
4. Aiaz, J.; Rubio, L. *Mater Process Technol* 2003, 143, 342.
5. He, J.; Wang, Y.; Zhang, H. *Compos Sci Technol* 2000, 60, 1919.
6. Martin, T. A.; Bhattacharyya, D.; Collins, I. F. *Compos Manuf* 1995, 6, 177.
7. Meng, Y. Z.; Tjong, S. C.; Hay, A. S. *Polymer* 1998, 39, 1845.
8. Xigao, J.; Yuezhong, M.; Haibin, Z.; Hay, A. S. The preparation of Poly(Ether Sulfone)s Containing Phthalazone Moieties, China Pat. CN93109179.9 (1993).
9. Xigao, J.; Yuezhong, M.; Haibin, Z.; Hay, A. S. The preparation of Poly(Ether Ketone)s Containing Phthalazone Moieties, China Pat. CN93109180.2 (1993).
10. Xigao, J.; Ping, C.; Gongxiong, L. *Acta Polym Sin* 2003, 8, 469.
11. Meng, Y. Z.; Hay, A. S.; Jian, X. G.; Tjong, S. C. *J Appl Polym Sci* 1997, 66, 1425.
12. Guanghong, L.; Hongde, X. U.; Xigao, J. *Insulating Mater Commun* 1997, 5, 31.
13. Hoecker, F.; Karger-Kocsis, J. *J Appl Polym Sci* 1996, 59, 139.
14. Wu, G. M. *Mater Chem Phys* 2004, 85, 81.
15. Lee, Y.-S.; Lee, B.-K. *Carbon* 2002, 40, 2461.
16. Saihi, D.; El-Achari, A.; Ghenaim, A. *Polym Test* 2002, 21, 615.
17. Park, J.-M.; Kim, D.-S.; Kim, S.-R. *J Colloid Interface Sci* 2003, 264, 431.
18. Ping, C.; Chun, L.; Qi, Y. *Chin J Mater Res* 2005, 19, 159.
19. Jinfang, Z.; Shengru, Q.; Zheming, Q. *Fiber Reinforced Plast Compos* 1994, 4, 37.
20. Huiling, G.; Weihong, Z.; Zuoguang, Z. *Acta Mater Compos Sin* 2001, 18, 38.
21. Zhao, Q.; Liu, Y.; Abel, E. W. *J Colloid Interface Sci* 2004, 280, 174.
22. Adams, R. D.; Singh, M. M. *Compos Sci Technol* 1996, 56, 977.
23. Selzer, R.; Friedrich, K. *Composites* 1997, 28, 595.
24. Cervenka, A. J.; Bannister, D. J.; Young, R. J. *Compos A* 1998, 29, 1137.
25. Lundgren, J.-E.; Gudmundson, P. *Compos Sci Technol* 1999, 59, 1983.
26. Kumosa, L.; Benedikt, B.; Armentrout, D.; Kumosa, M. *Compos A* 2004, 35, 1049.
27. Vlasveld, D. P. N.; Parlevliet, P. P.; Bersee, H. E. N. *Compos A* 2005, 36, 1.
28. Ye, L.; Afaghi-Khatibi, A.; Lawcock, G. *Compos A* 1998, 29, 1525.